Numerical Analysis of Gas Flows in Microchannels in Series

[1]Chan Hong Chung*(School of Food, Bio & Chemical Eng., Daegu Univ.)

직렬 미소채널 기체유장의 수치해석

정찬홍[1](대구대학교 식품·생명·화학공학부)
chc@webmail.daegu.ac.kr

ABSTRACT

A kinetic theory analysis is made of low-speed gas flows in a microfluidic system consisted of three microchannels in series. The Boltzmann equation simplified by a collision model is solved by means of a finite difference approximation with the discrete ordinate method. For the evaluation of the present method results are compared with those from the DSMC method and an analytical solution of the Navier-Stokes equations with slip boundary conditions. Calculations are made for flows at various Knudsen numbers and pressure ratios across the channel. The results compared well with those from the DSMC method. It is shown that the analytical solution of the Navier-Stokes equations with slip boundary conditions which is suited for fully developed flows can give relatively good results in predicting the geometrically complex flows up to a Knudsen number of about 0.06. It is also shown that the present method can be used to analyze extremely low-speed flow fields for which the DSMC method is impractical.

Keywords : MEMS, Microchannel Flow, Boltzmann Equation, BGK Model, Discrete Ordinate Method, Finite Difference Method

Nomenclatures

A_c : collision frequency
d : characteristic length
F : local equilibrium distribution
f : number density distribution function
G, H : reduced equilibrium distribution
g, h : reduced distribution function
L : length of channel
Kn : Knudsen number, λ / d
m : mass of molecule
n : number density
n_w : wall number flux
P : pressure
R : gas constant
T : temperature
U : macroscopic flow velocity
V : molecular velocity
Y : height of channel

λ : molecular mean free path
μ : coefficient of viscosity
ω : VHS exponent
ψ : BGK model constant

1. Introduction

Microchannels are important components of micro-electro-mechanical systems(MEMS) which have been the subject of increasingly active research during the last three decades. The length scale of microchannels in MEMS devices is typically on the order of microns. The Knudsen number of the flow field, the ratio of the mean free path to the characteristic channel dimension, is usually not negligibly small even at atmospheric operating conditions. Hence, conventional computational fluid dynamics (CFD) methods which are based on continuum assumptions may not be appropriate and a method based on kinetic gas theory is required to describe the flows accurately.

Of the various methods available for the analysis of microchannel flows, the direct simulation Monte-Carlo (DSMC) method [1] has been used by many researchers [2-6]. The DSMC method has been known to be a robust and accurate method because it is based on kinetic gas theory and does not rely on the continuum assumption that is not valid for high Knudsen

number gas flows. Even though the DSMC method has been successfully applied for the analysis of various kind of rarefied gas flows, simulation of low-speed microchannel flows using the DSMC method suffers from several difficulties including large statistical scatter that has not been encountered in the high speed gas flow simulations. To get a meaningful result by reducing the large statistical noise, the DSMC method requires huge amount of computational effort due the number of time steps to reach the steady-state flow condition and the large number of sample size [4]. These computational demands can render the standard DSMC method impractical given current computing power limitations. Due to the difficulties, most of the reported DSMC simulations have been dealing with simple microchannels with very small length-to-height (L/H) ratio and relatively large pressure ratio.

In the present study a finite-difference method coupled with the discrete-ordinate method [7,8] is employed to analyze low-speed gas flows in a microfluidic system. In the method, Boltzmann equation simplified by a collision model (BGK equation) [9] is solved by means of a finite-difference approximation. The physical space is transformed by a general grid-generation technique. The velocity space is transformed to a polar coordinate and the concept of the discrete ordinate method is employed to discretize the velocity space. The modified Gauss-Hermite quadrature [10,11] and Simpson's rule are used for the integration of the discretized velocity space.

To assess the present method, calculations are made for flows inside a microfluidic system consisted of three microchannels in series. Results are compared with those from the DSMC method and an analytical solution of the Navier-Stokes equations with slip boundary conditions [12]. Calculations are made for flows at various Knudsen numbers from 0.06 to 10 and pressure ratios across the channel from 1.05 to 2.5.

2. Numerical Method

2.1 Model Equation

We consider the steady-state Boltzmann equation with the BGK model [9] in a two-dimensional Cartesian coordinate system

$$V_x \frac{\partial f}{\partial x} + V_y \frac{\partial f}{\partial y} = A_c (F - f) \qquad (1)$$

where $f(x, y, V_x, V_y, V_z)$ is the distribution function, x and y are Cartesian coordinates of the physical space, V_x, V_y, and V_z are the velocity components of the molecules, and A_c is the collision frequency. The equilibrium Maxwell-Boltzmann distribution F is given by

$$F = n(2\pi RT)^{-3/2} \exp[-(V-U)^2 / 2RT] \qquad (2)$$

The moments n, U, and T can be obtained by integrating the distribution function over the velocity space:

$$n = \int f \, dV \qquad (3a)$$

$$nU = \int V f \, dV \qquad (3b)$$

$$3nRT = \int (V-U)^2 f \, dV \qquad (3c)$$

where R denotes the gas constant, n the particle density, U the macroscopic flow velocity.

The following reduced distribution functions are introduced to reduce the number of independent variables:

$$g(x, y, V_x, V_y) = \int_{-\infty}^{+\infty} f(x, y, V_x, V_y, V_z) \, dV_z \qquad (4a)$$

$$h(x, y, V_x, V_y) = \int_{-\infty}^{+\infty} V_z^2 f(x, y, V_x, V_y, V_z) \, dV_z \qquad (4b)$$

These kinds of reduced distribution functions were first applied by Chu [13] and employed by many investigators. The corresponding equations for the reduced distribution functions are obtained by integrating out the V_z dependence with the weighting functions 1 and V_x^2, respectively:

$$V_x \frac{\partial g}{\partial x} + V_y \frac{\partial g}{\partial y} = A_c (G - g) \qquad (5a)$$

$$V_x \frac{\partial h}{\partial x} + V_y \frac{\partial h}{\partial y} = A_c (H - h) \qquad (5b)$$

$$G(x,y,V_x,V_y) = \int_{-\infty}^{+\infty} F \, dV_z \qquad (5c)$$

$$H(x,y,V_x,V_y) = \int_{-\infty}^{+\infty} V_z^2 F \, dV_z \qquad (5d)$$

Using the characteristic length of a flow field d and the most probable speed V_o defined as

$$V_o = \sqrt{2RT_o} \qquad (6)$$

the following dimensionless variables are introduced:

$$\hat{x} = x/d \;,\; \hat{y} = y/d \;,\; \hat{n} = n/n_o \;,\; \hat{V}_i = V_i/V_o \;,$$
$$\hat{U}_i = U_i/V_o \;,\; \hat{T}_i = T_i/T_o \;,\; \hat{A}_c = \hat{A}_c d/V_o \;,$$
$$\hat{g} = gV_o^2/n_o \;,\; \hat{h} = h/n_o \;,\; \hat{G} = GV_o^2/n_o \;,$$
$$\hat{H} = H/n_o \;,\; \hat{\tau} = \tau/(1/2mn_oU_\infty^2) \qquad (7)$$

where the subscript $_o$ refers to a reference condition.

By introducing a polar coordinate system, which is defined as

$$\hat{V}_x = V\sin\phi \qquad (8a)$$

$$\hat{V}_y = V\cos\phi \qquad (8b)$$

$$\phi = \tan^{-1}(\hat{V}_x/\hat{V}_y) \qquad (8c)$$

and applying general transform rules, the governing equations in the new coordinate system (ξ,η) are written as [7]

$$B\frac{\partial\hat{g}}{\partial\eta} + C\frac{\partial\hat{g}}{\partial\xi} = \hat{A}_c(\hat{G}-\hat{g}) \qquad (9a)$$

$$B\frac{\partial\hat{h}}{\partial\eta} + C\frac{\partial\hat{h}}{\partial\xi} = \hat{A}_c(\hat{H}-\hat{h}) \qquad (9b)$$

$$B = (\hat{x}_\xi\cos\phi - \hat{y}_\xi\sin\phi)\; V/J_t \qquad (9c)$$

$$C = (\hat{y}_\eta\sin\phi - \hat{x}_\eta\cos\phi)\; V/J_t \qquad (9d)$$

Here, J_t denotes the Jacobian of the transformation.

2.2 Discrete Ordinate Method

In order to remove the velocity-space dependency from the reduced distribution functions, the discrete ordinate method [7,8] is employed. This method, which consists of replacing the integration over velocity space of the distribution functions by appropriate integration formulas, requires the values of the distribution functions only at certain discrete speeds and velocity angles. Employing discrete distribution functions $\hat{g}_{\delta\sigma}(\xi,\eta,V_\delta,\phi_\sigma)$ and $\hat{h}_{\delta\sigma}(\xi,\eta,V_\delta,\phi_\sigma)$ for the discrete speed V_δ and velocity angle ϕ_σ, the macroscopic moments given by integrals over the molecular velocity space can be substituted by the following quadratures:

$$\hat{n} = \sum_\delta\sum_\sigma P_\delta P_\sigma \hat{g}_{\delta\sigma} \qquad (10a)$$

$$\hat{n}\hat{U}_x = \sum_\delta\sum_\sigma P_\delta P_\sigma V_\delta \sin\phi_\sigma \hat{g}_{\delta\sigma} \qquad (10b)$$

$$\hat{n}\hat{U}_y = \sum_\delta\sum_\sigma P_\delta P_\sigma V_\delta \cos\phi_\sigma \hat{g}_{\delta\sigma} \qquad (10c)$$

$$3\hat{n}\hat{T}/2 = \sum_\delta\sum_\sigma P_\delta P_\sigma (h_{\delta\sigma} + V_\delta^2 \hat{g}_{\delta\sigma})$$
$$-\hat{n}(\hat{U}_x^2 + \hat{U}_y^2) \qquad (10d)$$

where P_δ and P_σ are weighting factors of the quadratures for the discrete speed V_δ and velocity angle ϕ_σ, respectively. Thus instead of solving the equations for a function of space and molecular velocity, the equations are transformed to partial differential equations, which are continuous in space but are point functions in molecular speed, V_δ, and velocity angle, ϕ_σ, as follows:

$$B_{\delta\sigma}\frac{\partial\hat{g}_{\delta\sigma}}{\partial\eta} + C_{\delta\sigma}\frac{\partial\hat{g}_{\delta\sigma}}{\partial\xi} = \hat{A}_c(\hat{G}_{\delta\sigma} - \hat{g}_{\delta\sigma}) \qquad (11a)$$

$$B_{\delta\sigma}\frac{\partial\hat{h}_{\delta\sigma}}{\partial\eta} + C_{\delta\sigma}\frac{\partial\hat{h}_{\delta\sigma}}{\partial\xi} = \hat{A}_c(\hat{H}_{\delta\sigma} - \hat{h}_{\delta\sigma}) \qquad (11b)$$

$$B_{\delta\sigma} = (\hat{x}_\xi\cos\phi_\sigma - \hat{y}_\xi\sin\phi_\sigma)\; V_\delta/J_t \qquad (11c)$$

$$C_{\delta\sigma} = (\hat{y}_\eta\sin\phi_\sigma - \hat{x}_\eta\cos\phi_\sigma)\; V_\delta/J_t \qquad (11d)$$

2.3 Collision Frequency

The simplest model for the collision integral is the BGK model [9] which has been widely used and generally gives reasonable results with much less computational effort. In the BGK model the collision frequency is given by

$$A_c = \psi \frac{P}{\mu} \tag{12}$$

where the quantity ω is the viscosity index, and ψ is a numerical parameter. The coefficient of viscosity, μ, is assumed to have a temperature dependency [14]

$$\frac{\mu}{\mu_o} = \left(\frac{T}{T_0}\right)^{\omega} \tag{13}$$

The equilibrium mean free path for the VHS model [15] is employed

$$\lambda_o = \frac{16}{5} \frac{F_k \mu_o}{m n_o \sqrt{2\pi R T_o}} \tag{14}$$

where the quantity F_c is given by

$$F_k = \frac{(5-2\omega)(7-2\omega)}{24} \tag{15}$$

Combining Eqs. (12) to (15), we obtain

$$\hat{A}_c = \frac{8\psi F_k \hat{n} \hat{T}^{1-\omega}}{5\sqrt{\pi} Kn_o} \tag{16}$$

where Kn_o is the Knudsen number at the reference condition based on the characteristic length of the flow field, d.

2.4 Numerical Procedure

Equations (11a) and (11b) are solved by means of finite-difference approximations in physical space using simple explicit and implicit schemes depending on the characteristics of physical and velocity space. Details of the method can be found elsewhere [7]. Resulting system of nonlinear algebraic equations is solved by means of successive approximations. In the iterative procedure, only the values of $\hat{A}_c$, $\hat{G}_{\delta\sigma}$, and $\hat{H}_{\delta\sigma}$ have to be determined from moments of the previous iteration, and the values of distribution functions do not need to be stored. Convergence is assumed to have occurred when the relative differences in the x-velocities of two successive iteration steps are less than 10^{-5} for all spatial grid points. As a proper quadrature formula for the discrete speed V_δ, the modified Gauss-Hermite half range quadrature for integrals of the form [10,11] is used:

$$\int_0^\infty V^j \exp(-V^2)\, Q(V) dV = \sum_{\delta=1}^{N} P_\delta Q(V_\delta) \tag{17}$$

2.5 Boundary Conditions

The following boundary conditions are used for the calculation. At inlet and exit boundaries, the distribution functions are given by an equilibrium distribution with prescribed conditions:

$$f_b = n_b (2\pi R T_b)^{-3/2} \exp[-(V-U_b)^2 / 2RT_b] \tag{18}$$

where the subscript $_b$ refers to conditions at the boundaries.

In order to specify the interaction of the molecules with the surface, diffuse reflection is assumed, i.e., molecules that strikes the surface are subsequently emitted with a Maxwell distribution characterized by the surface temperature T_w:

$$f_w = n_w (2\pi R T_w)^{-3/2} \exp[-(V-U_w)^2 / 2RT_w]$$

$$\text{for} \quad (V \cdot \tilde{n}) < 0 \tag{19}$$

where the subscript $_w$ refers to conditions at the surface, $\tilde{n}$ is the inward normal vector to the surface. The wall number flux n_w is not known a priori, and may be determined by applying the condition of no net flux normal to the surface:

$$\int_{(V\cdot\tilde{n})>0} (V\cdot\tilde{n}) f dV = -\int_{(V\cdot\tilde{n})<0} (V\cdot\tilde{n}) f_w dV \tag{20}$$

3. Results and Discussion

We consider a two-dimensional microfluidic system consisted of 3 microchannels in series as shown in Fig. 1. The gas is air with the viscosity index of $\omega = 0.77$. The pressures at the inlet and the exit are 2.5×10^5 and 1.0×10^5 Pa, respectively. The temperature at the inlet is 300K. The diffuse boundary condition at the wall temperature of 300K is used. The coefficient of viscosity and the reference molecular diameter of air are assumed to be $\mu = 1.791\times10^{-5}\ N\cdot s/m^2$ and $d_{ref} = 4.20$ Å, respectively. The average Knudsen number calculated using the flow variables at the mean pressure $P = (P_o + P_d)/2$ is

Kn = 0.06. The exponent j and the order of the quadrature N in Eq. (17) are chosen to be 1 and 16, respectively. Simpson's $3/8th$ rule with $\Delta\phi = \pi/30$ is used for the discrete velocity angle. The BGK model parameter ψ was chosen to be 1.3 for the problems considered in the present study. In case of the hard sphere molecules the BGK model parameter ψ usually assumed to be between 2/3 and 1 [16] from the well known behavior of the BGK model, which needs further investigation.

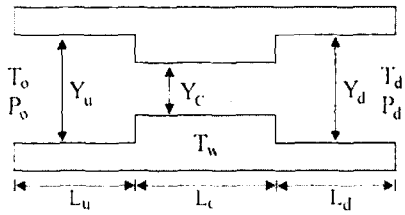

Fig. 1. Geometry of a microfluidic system consisted of 3 microchannels in series.

Table 1: Summary of parameters

L_u, L_d	7.5 μm
L_c	15 μm
Y_u, Y_d	1.0 μm
Y_c	0.5 μm
T_o, T_d, T_w	300K

To check the accuracy of the present method, the results are compared with those from the DSMC method and the analytical solution of the Navier-Stokes equations with slip boundary conditions [12].

The DSMC code used in the present study is based on the same principles as described in Bird [1], together with the variable hard sphere (VHS) model [15] as a molecular model and the no time counter (NTC) method [17] as a collision sampling technique. The code has been applied to various low-density flows of gas mixtures in arbitrary shaped flow domains [18,19]. Details of the code may be found in Ref. 18.

At the inlet and outflow boundaries, the pressure boundary condition adopted by Nance *et. al.* [5] is used to correct the variables at the boundaries both for the present and the DSMC methods. For the calculations only upper half portion of the flow domain is considered with a symmetric boundary condition along the centerline. For the DSMC calculation, a rectangular grid system of 24,000 (160x50+ 320x25+160x50) cells is employed with ca. 1,040,000 particles and 75,000 sampling time steps(average sampling size of ca. 3.2×10^6 per cell) after 50,000 time steps of development. For the present method a rectangular grid system of 161x51+ 321x26+160x51 grids is employed. CPU times required for the DSMC and the present methods were ca. 116 and 39hrs, respectively. All the calculations in the present work are performed on a desktop computer with a Pentium IV 3.2GHz processor.

Details of the analytical solution of the Navier-Stokes equations may be found in Ref. 12. In the method the Navier-Stokes equations are solved for a long 2-D isothermal channel in the slip flow regime with slip boundary conditions

$$U_{wall} = \theta\lambda\left(\frac{\partial U}{\partial y}\right)_{wall} \tag{19}$$

where the quantity θ represents the streamwise momentum accommodation

$$\theta = \frac{2-\theta_m}{\theta_m} \tag{20}$$

and θ_m is the tangential momentum coefficient, which varies from zero (specular or zero accommodation) to one (full accommodation):

$$\overline{P}(\bar{x}) = \sqrt{(6\theta K_e + R_P)^2 - \bar{x}[(R_P^2 - 1) + 12\theta K_e(R_P - 1)]} - 6\theta K_e \tag{21}$$

$$U(x,y) = \frac{1}{2\mu}\frac{dP}{dx}\left(y^2 - Y_o^2 - 4Y_o^2 K\theta\right) \tag{22}$$

where x and y are the streamwise distances from the inlet and the lateral distance from the centerline, respectively; $\overline{P}$ and $\bar{x}$ are nondimensionalized pressure and x distance normalized by the exit pressure and the channel length, respectively; $U(x,y)$ is x-velocity; subscript $_e$ represents a value at the exit; the tangential momentum coefficient θ_m was set to be 0.85 to fit experimental results [6]. In the equations, K is a Knudsen number given by:

$$K = \sqrt{\frac{\pi\gamma}{2}}\frac{Ma}{\mathrm{Re}} \tag{23}$$

where Ma is Mach number, Re is Reynolds number, and γ is the ratio of specific heats.

Figures 2 and 3 show the comparison of x-velocity and pressure contours, respectively, obtained by the present and the DSMC methods. The contours in the upper half portion of the figure are results of the present method and those in the lower half portion are results calculated by the DSMC method. In the figures the unit of velocity is m/s and the pressure is nondimensionalized by the inlet pressure P_o. The variation of x-velocity in the streamwise direction is very small at the first and third channels and the most of the pressure drop occurs in the second channel. The variation of pressure in the lateral direction is negligible. It can be seen that the pressure at the location x/L = 0.5 is larger than the mean pressure 0.7.

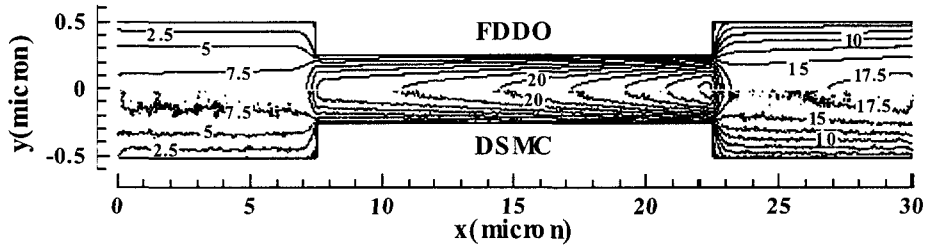

Fig. 2. Comparison of x-velocity contours for P_o/P_d = 2.5 and Kn = 0.06.

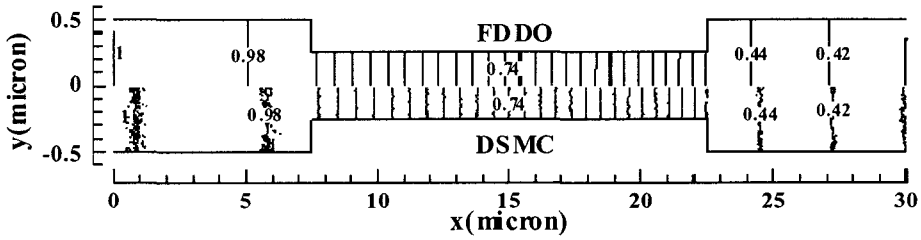

Fig. 3. Comparison of pressure contours for P_o/P_d = 2.5 and Kn = 0.06.

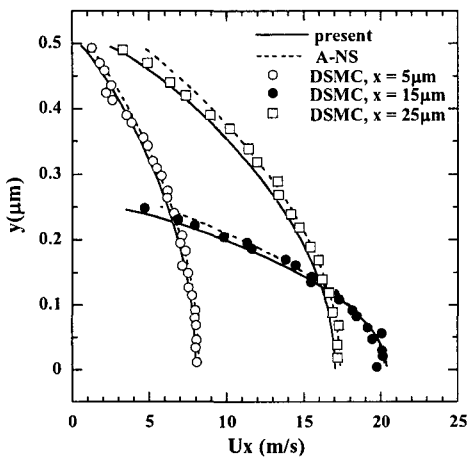

Fig. 4. Comparison of x-velocity distributions along the centerline for P_o/P_d = 2.5 and Kn = 0.06.

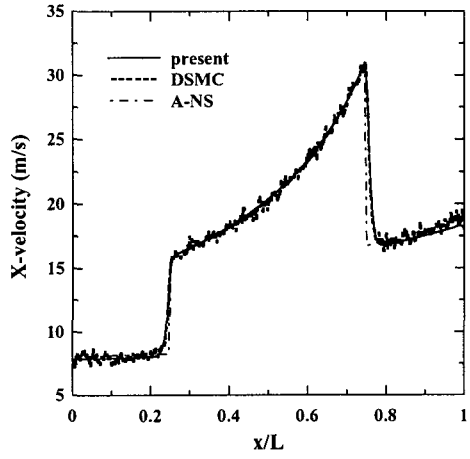

Fig. 5. Comparison of x-velocity distributions along the centerline for P_o/P_d = 2.5 and Kn = 0.06.

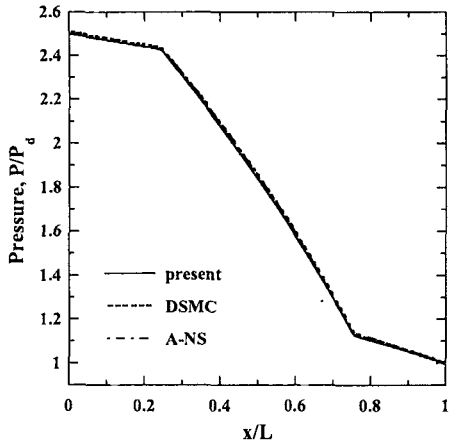

Fig. 6. Comparison of pressure distributions along the centerline for P_o / P_d = 2.5 and Kn = 0.06.

Figure 4 shows x-velocity profiles at x = 5, 10, and 15 μm from the present and the DSMC methods together with those from the analytical solution of the Navier-Stokes equations with slip boundary conditions(A-NS). The results for the analytical solution of the Navier-Stokes equations with slip boundary conditions are obtained by assuming the pressures at the junctions and the mass fluxes through the three channels are equal, which means entrance and exit effects are neglected. It can be seen that the results from the present method compare very well with those from the DSMC method. The results from the analytical solution of the Navier-Stokes equations compare relatively well except for some differences near the surface.

Figures 5 and 6 compare x-velocity and pressure distributions, respectively, along the centerline of the channel from three different methods. The flow remains slow in the first channel, accelerates through the second channel, and the velocity drops sharply at the entrance of the third channel where the flow expands. It can be seen that the results from the present and the DSMC methods compare very well.

The velocity distribution from the Navier-Stokes equations with slip boundary conditions shows relatively good agreement except at the junctions due to entrance and exit effects. There were little differences among the pressure distributions obtained by the three different methods. It is very interesting to see that the analytical solution of the Navier-Stokes equations with slip boundary conditions which is suited for fully developed flows can give relatively good results in predicting the geometrically complex flows.

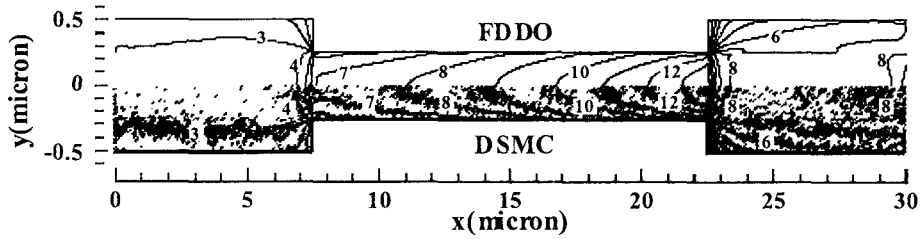

Fig. 7. Comparison of x-velocity contours for P_o / P_d = 2.5 and Kn = 10.

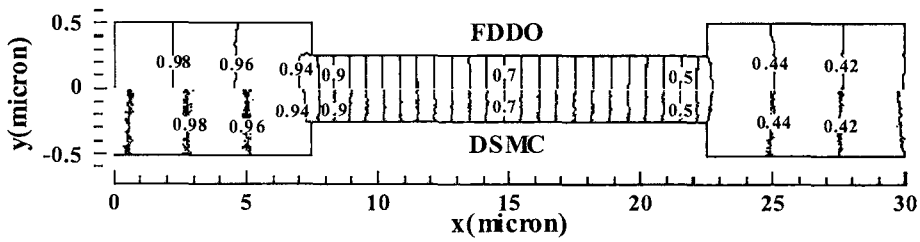

Fig. 8. Comparison of pressure contours for P_o / P_d = 2.5 and Kn = 10.

To check the accuracy of the present method at free-molecular flow regimes, calculations are made for a flow at an average Knudsen number Kn = 10 by reducing the inlet and exit pressures while keeping the pressure ratio P_o / P_d = 2.5.

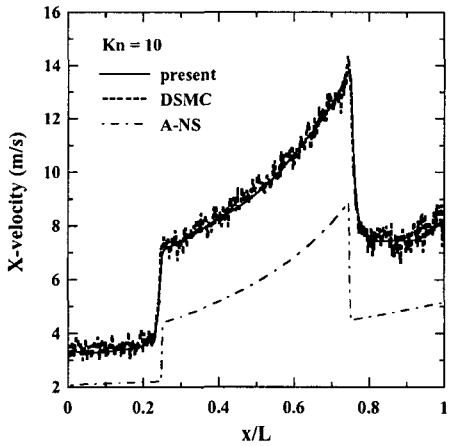

Fig. 9. Comparison of x-velocity distributions along the centerline for P_o / P_d = 2.5 and Kn = 10.

Figures 7 and 8 show the comparison of x-velocity and pressure contours, respectively, at Kn = 10 obtained by the present and the DSMC methods. The contours in the upper half portion of the figure are results of the present method and those in the lower half portion are results calculated by the DSMC method. It can be seen that the results from the present and the DSMC methods compare well except for the large statistical scatter in the x-velocity contours obtained by the DSMC method. It also can be seen that the flow is much slower than that of Kn = 0.06. Figure 9 compares x-velocity distributions along the centerline of the channel from the three different methods. It can be seen that the results from the present and the DSMC methods compare very well. As expected, the velocity distribution from the analytical solution of the Navier-Stokes equations with slip boundary conditions shows poor agreement since the method is based on the continuum assumptions.

To investigate the applicability of the analytical solution of the Navier-Stokes equations with slip boundary conditions, x-velocity distributions along the centerline of the channel are compared with those from the present method at Knudsen numbers Kn = 0.06, 0.1, and 0.5 as shown in Fig. 10. It should be noted that Kn = 0.1 is the boundary between the slip and transition flow regimes. It can be seen that as Knudsen number increases the difference in the velocity distributions increases, which implies that ca. Kn = 0.06 is the highest Knudsen number the Navier-Stokes equations with slip boundary conditions can be used.

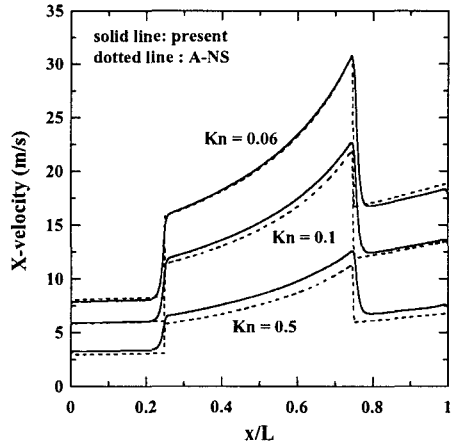

Fig. 10. Comparison of x-velocity distributions along the centerline at slip and transition flow regimes for P_o / P_d = 2.5.

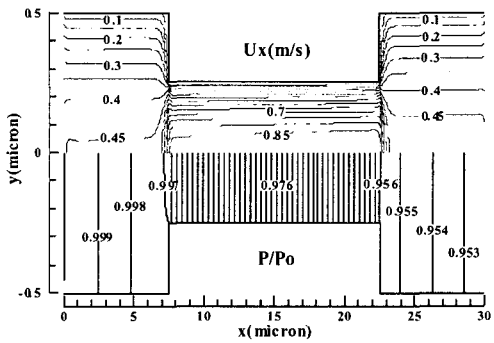

Fig. 11. X-velocity and pressure contours for P_o / P_d = 1.05 and Kn = 0.06.

It is well known that the DSMC method requires huge amount of computational effort to get a meaningful result by reducing the large statistical noise in the simulation of low-speed flows [4]. These computational demands can render the standard DSMC method impractical given current computing power limitations. The present method does not suffer from the statistical

noise and can be used for the simulation of extremely low-speed flows. To assess the feasibility of the present method at low speed flows, calculations are made for flows through the channel with several different pressure ratios. Figure 11 shows x -velocity and pressure contours in the channel for a pressure ratio of P_o / P_d = 1.05. The contours in the upper half portion of the figure are x-velocity contours and those in the lower half portion are pressure contours. The variation of x -velocity in the streamwise direction is very small and the variation of pressure in the lateral direction is negligible. It can be seen that the pressure at the location x/L = 0.5 almost equals to the mean pressure 0.976.

The magnitude of x -velocity in the first channel are less than or equal to 0.45 m/s . If the DSMC method is employed and a 3% noise is allowed(see Fig. 2), the required sample size would be ca. 9.5×10^8 per cell. The required CPU time for the DSMC method would be ca. 34,800 hrs(or ca. 4 years) on the Pentium IV 3.2GHz PC used in the present study. The required CPU time for the present method was ca. 41hrs using the converged solution of the case of P_o / P_d = 2.5 as an initial guess.

Figure 12 shows x -velocity distributions along the centerline of the channel for several different pressure ratios from P_o / P_d = 1.05 to 2.5. The velocity distributions from the present method and the Navier-Stokes equations with slip boundary conditions show relatively good agreement except at the junction due to entrance and exit effects. Figure 13 shows centerline x-velocities from the present and and the Navier-Stokes equations with slip boundary conditions at x/L = 0.1, 0.5, and 0.9. The results from the two methods are in good agreement.

4. Conclusions

A finite-difference method coupled with the discrete-ordinate method is employed to analyze low-speed gas flows in a microfluidic system consisted of three microchannels in series. For the evaluation of the present method results are compared with those from the DSMC method and an analytical solution of the Navier-Stokes equations with slip boundary conditions. Calculations are made for flows at various Knudsen numbers from 0.06 to 10 and pressure ratios across the channel from 1.05 to 2.5. The results compared well with those from the DSMC method. It is shown that the analytical solution of the Navier-Stokes equations with slip boundary conditions which is suited for fully developed flows can give relatively good results in predicting the geometrically complex flows up to a Knudsen number of about 0.06. The advantage of the present method is that it does not suffer from statistical noise which is common in particle based methods. It is shown that the present method can be used to analyze low-speed flows that would be almost impossible for the DSMC method.

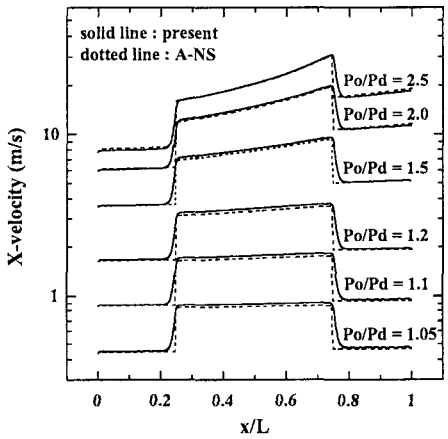

Fig. 12. Comparison of x-velocity distributions along the centerline at several pressure ratios across the channel at Kn = 0.06.

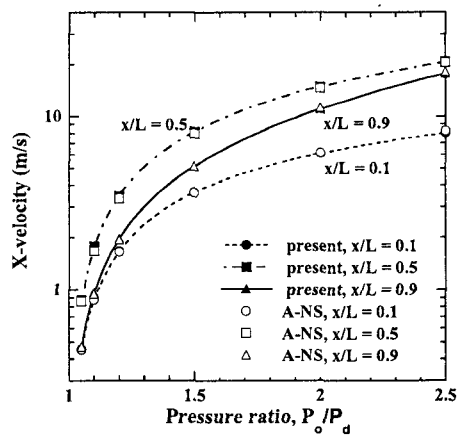

Fig. 13. Effect of pressure ratio on the centerline velocity at Kn = 0.06.

Acknowledgments

This work was support(in part) by grant No. R05-2003-000-10145-0 from the Basic Research Program of the Korea Science & Engineering Foundation.

References

1. Bird, G. A., Molecular Gas Dynamics and the Direct Simulation of Gas Flows, Clarendon, Oxford, 1994.

2. Ikegawa, M., and Kobayashi, J., "Development of a Rarefied Flow Simulator Using the Direct-Simulation Monte-Carlo Method," JSME International Journal, Series 2, Vol. 33, No. 3, 1990, pp. 463-467.

3. Piekos, E. S. and Breuer, K. S., "Numerical Modeling of Micromechanical Devices Using the Direct Simulation Monte-Carlo Method," Transactions of the ASME, Vol. 118, 1996, pp. 464-469.

4. Oh, C. K., Oran, E. S., and Sinkovits, R. S., "Computations of High-Speed, High Knudsen Number Microchannel Flows," Journal of Thermophysics and Heat Transfer, Vol. 11, No. 4, 1997, pp. 497-505.

5. Nance, P. R., Hash, D. B., and Hassan, H. A., "Role of Boundary Conditions in Monte Carlo Simulation of Microelectromechanical Systems," Journal of Thermophysics and Heat Transfer, Vol. 12, No. 3, 1998, pp. 447-449.

6. Cai, C., Boyd, I. D., Fan, J., and Candler, G. V., "Direct Simulation Methods for Low-Speed Microchannel Flows," Journal of Thermophysics and Heat Transfer, Vol. 14, No. 3, 2000, pp. 368-378.

7. Chung, C. H., De Witt, K. J., Jeng, D. R., and Keith Jr., T. G., "Numerical Analysis of Rarefied Gas Flow Through Two-Dimensional Nozzles," J. of Propulsion and Power, Vol. 11, No. 1, 1995, pp. 71-78.

8. Huang, A. B., "The Discrete Ordinate Method for the Linearized Boundary Value Problems in Kinetic Theory of Gases," Georgia Institute of Technology, School of Aerospace Engineering, Rarefied Gas Dynamics and Plasma Lab. Rept. 4, Atlanta, GA, 1967.

9. Bhatnagar, P. L., Gross, E. P., and Krook, M., "A Model for Collision Processes in Gases. I. Small Amplitude Processes in Charged and Neutral One-Component Systems," Physiacal Review, Vol. 94, No. 3, 1954, pp. 511-525.

10. Huang, A. B., and Giddens, D. P., " A New Table for a Modified (Half-Range) Gauss-Hermite Quadrature with an Evaluation of the Integral," Journal of Mathematics and Physics, Vol. 47, 1968, pp. 213-218.

11. Shizgal, B., "A Gaussian Quadrature Procedure for Use in the Solution of the Boltzmann Equation and Related Problems," Journal of Computational Physics, Vol. 41, No. 2, 1981, pp. 309-328.

12. Arkilic, E. B., Schmidt, M. A., and Breuer, K. S., "Gaseous Slip Flow in Long Microchannels," Journal of Microelectromechanical Systems, Vol. 6, No. 2, 1977, pp. 167-178.

13. Chu, C. K., "Kinetic-Theoretic Description of the Formation of a Shock Wave," Physics of Fluids, Vol. 8, No. 1, 1965, pp. 12-22.

14. Chapman, S. and Cowling, T. G., The Mathematical Theory of Non-Uniform Gases, Cambridge University Press, London, 1958.

15. Bird, G. A., "Monte Carlo Simulation in an Engineering Context," Progress in Astronautics and Aeronautics: Rarefied Gas Dynamics, edited by Sam S. Fisher, Vol. 74, Part I, AIAA, New York, 1981, pp. 239-255.

16. Atassi, H. and Shen, S. F., "A Unified Kinetic Theory Approach to External Rarefied Gas Flows. Part 1. Derivation of Hydrodynamic Equations," Journal of

Fluid Mechanics, Vol. 53, Part 3, 1972, pp. 417-431.

17. Bird, G. A., "The Perception of Numerical Methods in Rarefied Gas Dynamics," *Progress in Astronautics and Aeronautics: Rarefied Gas Dynamics*, edited by E. P. Muntz, D. P. Weaver, and D. H. Campbell, AIAA, Washington, DC, Vol. 118, 1989, pp. 211-226.

18. Chung, C. H., De Witt, K. J., Stubbs, R. M., and Penko, P. F., "Simulation of Overexpanded Low-Density Nozzle Plume Flow," AIAA J., Vol. 33, No. 9, 1995, pp. 164-1650.

19. Chung, C. H., Kim, S. C., De Witt, K. J., and Nagamatsu, H. T., "Numerical Analysis of Hypersonic Low-Density Scramjet Inlet Flow," J. Spacecraft and Rockets, Vol. 32, No. 1, 1995, pp. 60-66.